Electric-Field Control of Magnetism in Graphene Quantum Dots: Ab Initio Calculations

Published in final edited form as:
Phys Rev B Condens Matter Mater Phys. 2010 November 23; 82(20): 201411–.

Electric-field control of magnetism in graphene quantum dots: *Ab initio* calculations

Luis A. Agapito[1], **Nicholas Kioussis**[1], and **Efthimios Kaxiras**[2]

[1]Department of Physics, California State University, Northridge, California 91330-8268, USA

[2]Department of Physics and School of Engineering and Applied Sciences, Harvard University, Cambridge, Massachusetts 02138, USA

Abstract

Employing *ab initio* calculations we predict that the magnetic states of hydrogenated diamond-shaped zigzag graphene quantum dots (GQDs), each exhibiting unique electronic structure, can be selectively tuned with gate voltage, through Stark or hybridization electric-field modulation of the spatial distribution and energy of the spin-polarized molecular orbitals, leading to transitions between these states. Electrical read-out of the GQD magnetic state can be accomplished by exploiting the distinctive electrical properties of the various magnetic configurations.

The relentless drive to produce ever faster and more complex electronic devices has led to features that are quickly approaching atomic-size scale. Few physical systems can be manipulated at this scale to produce reliably robust structures with the required electronic properties. Graphene, a single plane of threefold coordinated carbon atoms, exhibits[1] many exotic electronic properties ranging from highly mobile ballistic transport[2,3] to the Klein paradox.[4] Graphene nanoscale ribbons and patches exhibit magnetic properties of great interest and importance for technological applications in carbon-based spintronic devices that employ magnetic rather than charge degrees of freedom.[5-9] Extended systems, such as zigzag graphene nanoribbons (GNRs), display ferromagnetic (FM) or antiferromagnetic (AF) ordering between opposite edges. Recent predictions have shown that application of an electric field in hydrogenated zigzag GNRs can induce half metallicity,[5,6,9-11] where GNRs act as spin filters.

Molecular systems, such zigzag graphene quantum dots (GQDs) of triangular shape also exhibit a net magnetization[9,12,13] and could potentially be components of superstructures[14] acting as single-molecule spintronic devices; for instance, the magnetic ordering between individual triangular GQDs could be used to perform logic operations. GQDs, in particular, hold the promise of extremely long spin relaxation and decoherence times due to the very small spinorbit and hyperfine coupling in carbon.[15] However, this issue remains controversial and unresolved since theory and experiment yield values for the relaxation time differing by several orders of magnitude.[15] Among the most intriguing and promising uses of graphene is an all-carbon nanoscale spintronic device, which could actually fulfill the quest to design and build smaller and faster computers. Suggestions already exist for the fabrication of ultradense planar GQD-based devices carved entirely from graphene, in which a central nanopatch is connected through narrow constrictions to the source and drain ribbon contacts with side-gate electrodes to tune the dot charge.[16,17] The use of graphene ribbons as leads circumvents the need for external metallic contacts, which introduce notorious interface-related problems. Manipulation of the spin states of the GQD by purely local electrical rather than magnetic field means is of fundamental importance for the operation of spintronic devices such as spin filters, spin transistors, and magnetic memories, as well as for solid-state qubits, because the former are easier to generate through local gate electrodes;

this would also allow greater spatial selectivity, important for addressing of individual GQDs. Interestingly, recent *ab initio* electronic structure calculations have shown[18] that nonhydrogenated zigzag GNRs undergo a spontaneous planar reconstruction with a concomitant loss of magnetism while the hydrogenated unreconstructed zigzag GNRs are more stable and magnetic. Even though the fabrication of graphene nanostructures with well-defined edges has posed considerable technological challenge, recent experimental progress has shown a viable route for the fabrication of sharp edges[19] mostly with either zigzag or armchair edge and confirmed their stability.[20]

In this Rapid Communication we demonstrate that diamond-shaped graphene nanopatches (DGNs), with hydrogenated zigzag edges classified by the number of sites n, exhibit several remarkable and important properties which render them promising spintronic devices. Employing first-principles electronic-structure calculations we demonstrate that the AF, FM, and nonmagnetic (NM) states of DGNs can be controlled selectively by an external electric field. The underlying mechanism is the manipulation of the nature and the energies of the spin-polarized molecular orbitals (MO) through the field, on which the lowest energy magnetic state depends critically. Furthermore, each magnetic state is associated with very different electrical conductance, which may be pertinent to the ON/OFF switching reported recently by experiments.[17]

The first-principles density-functional calculations in the presence of uniform electric field were performed using the SIESTA method.[21] The valence electrons are expanded in terms of a double-ζ-polarized localized basis and the Troullier-Martin pseudopotentials are used for the core electrons. The generalized-gradient Perdew-Burke-Ernzerhof (PBE) exchange-correlation functional[22] and large cut-off energies (>300 Ry) for the mesh grid were employed.

In the absence of an electric field, the hydrogenterminated zigzag DGNs have an AF (net spin S_z=0) ground state, similar to zigzag GNRs. The first and second excited states are the FM and NM configurations. An important property of the diamond structure is that the energy difference between the AF ground state and the NM (FM) excited state increases linearly (remains constant at ≈150 meV) with size. The spin-polarized density of states (DOSs) for the AF, FM, and NM configurations of the n=8 DGN are shown in Figs. 1(a)–1(c), respectively, where the blue (red) curves denote the spin-up (spin-down) states, and the two panels for the AF state represent the projection of the DOS on the upper and lower triangle, respectively. The highest occupied molecular orbital-lowest unoccupied molecular orbital (HOMO-LUMO) energy gap of 0.66 eV for the AF configuration decreases to 0.27 eV for the FM and to 0.01 eV for the NM configuration. The FM and NM states, with smaller energy gaps, are expected to have high electrical conductance (ON or “1”), whereas the AF state is the low-conductance state (OFF or “0”). Interestingly, the DOS and spin density of the DGN in the AF state, projected on the upper and lower triangles, are similar to those of the isolated triangles,[13] indicating a weak intertriangular coupling.

The left vertical panels in Fig. 2 show the low-field ($\boldsymbol{E} < \boldsymbol{E}_{1c}$≈0.25 V/Å) evolution of the frontier MO energies for the AF (lower), FM (middle), and NM (upper) states, respectively, of the n=5-DGN. The field $\vec{E}$, shown in the inset, is coplanar with the DGN and applied along the larger diagonal of the DGN. The thick brown, green, and black background curves represent the schematic field variation in the corresponding total energy of the AF, FM, and NM states, showing that at the critical field, $\boldsymbol{E}_{1c}$≈0.25 V/Å, the DGN undergoes a FM→NM transition, with the eigenstates and total energies of the two configurations becoming identical. As discussed below, the DGN can be driven into its excited FM state via an increase in the field above the second critical field of 0.47 V/Å, followed by a rapid field quenching. The linear variation in the electric potential with distance across the DGN

decreases (increases) the electrostatic potential energy of the electrons in the lower (upper) triangle, leading to a linear Stark shift of both the HOMO and LUMO energies in the AF state for $\boldsymbol{E}$<0.1 V/Å. The central vertical panels in Fig. 2 show the intermediate-field (0.25<$\boldsymbol{E}$<0.47 V/Å) variation in the frontier MO energies for the AF and NM states, respectively, showing that the DGN undergoes an AF→NM transition at the critical field $\boldsymbol{E}_{2c}$ ≈0.47 V/Å, shown by the crossover of the red and black thick curves. For $\boldsymbol{E}$>$\boldsymbol{E}_{2c}$ the DGN remains in its NM state (right vertical panel in Fig. 2) loosing memory of its initial magnetic state. Depending on the rate of change of electric field the reverse NM→AF or NM → FM transitions may also take place depending on the transition energy barriers between the various magnetic states, which are beyond the scope of the present work. A slow (sudden) reduction of $\boldsymbol{E}$ below $\boldsymbol{E}_{2c}$ may (not) allow for sufficient electronic relaxation, driving the DGN to the AF (FM or NM) state at zero field.

In order to elucidate the underlying electronic mechanism of the electric-field switching of the GQDs magnetic state, we display in Figs. 3(a) and 3(b) the variation in the spinpolarized frontier MO energies with field for the AF and FM states, respectively. We also show schematically in Figs. 3(a) and 3(b) the field evolution of the corresponding spin-up (blue-shaded region) and spin-down (red-shaded area) frontier MO for the AF and FM states, respectively, where white denotes the absence of magnetization. At zero field, the spin-up (and spin-down, not shown here) HOMO and LUMO of the AF state are localized on opposite triangles, exhibiting *both* net electric polarization and spin magnetization. The electric polarization serves as an *electronic handle* through which the MO energies can be selectively tuned. The spatial asymmetry of the spin-polarized frontier MO gives rise to local magnetism with zero net spin. The electric field splits the initial double degeneracy of the energy levels of the AF-state which have constant field slope [left panel of Figs. 2 and 3(a)]. This is consistent with the linear Stark effect, where the shift of the MO energy, $\Delta E = -\vec{p}\cdot\vec{E}$, is proportional to its electric polarization $\vec{p}$. The HOMO ↑ (LUMO↑), localized on the upper (lower) triangles has an electric polarization antiparallel (parallel) to the field and hence its energy has a positive (negative) slope at low field ($\boldsymbol{E}$<0.1 V/Å). We find a similar trend for the doubly degenerate HOMO-1 and LUMO+1 levels (Fig. 2) but with a smaller field slope due to the weaker electric polarization of these MO. The energies of the nonpolar HOMO-2 and LUMO+2 (Fig. 2), are almost independent of field. The low-field behavior of the DGN in the AF state is the zero-dimensional analog of the half-metallic case predicted for one-dimensional GNR[5] but with the DGNs having the advantage of larger and more easily controllable band gap, which is important for electronic applications.

At higher fields ($\boldsymbol{E}$>0.1 V/Å), the field dependence of the frontier MO energies deviate from linearity, indicating a field-induced change of the polarization of the MO, that is, a quadratic Stark effect. In the dimerlike DGN, where the HOMO↑ and LUMO↑ are localized on opposite triangular subunits, the efficiency of electron flow from one subunit to the other, and hence the nonlinear effect, depends critically on the *interface* between the two subunits. The DGN proposed here allows for the most efficient charge transfer. The polarization (denoted by arrows) of the frontier spin-up MO decreases as the field increases, leading to the reduction in the slope of their energies in Fig. 3(a). Indeed at a field of ≈0.36 V/Å, the spin-up MO distribute symmetrically in both subunits, become nonpolar, and their field slopes vanish. At a field of ≈0.44 V/Å, the MO polarization, and hence the field slope of their energies, reverses, with a concomitant increase in the HOMO-LUMO gap. Further increase in the field leads to more transfer of the HOMO↑ to the bottom triangle where the HOMO↓ remains localized,[23] and becomes progressively similar to the HOMO↑. This spatial degeneracy induces energy degeneracy and the spin-up and spin-down MO energies begin to merge. Thus, at the critical field, $\boldsymbol{E}_{2c}$=0.47 V/Å, the local spin magnetization vanishes and the DGN undergoes a transition into the NM state. The actual *ab initio* results

for the electric-field variation in the spin-polarized frontier MO for the AF state shown in Fig. 4(a) corroborate this underlying electronic mechanism.

In sharp contrast, the zero-field spin-up (blue) and spindown (red) frontier MO for the FM configuration, shown in Fig. 3(b), are nonpolar. Nevertheless, the magnetism of this state can be still manipulated by a field, which, however, is of different origin. For $\boldsymbol{E}$<0.08 V/Å, the hybridization of nonpolar orbitals of *opposite* parity leads to the repulsion of the spin-down LUMO and LUMO+2 energies and the spin-up HOMO and HOMO-2 energies in Fig. 3(b) and the formation of polar bonding and antibonding MO. Namely, the zero-field spin-up HOMO and HOMO-2, shown in Fig.4(b), hybridize as the field is increased progressively, forming bonding (+) and antibonding (−) orbitals. The constructive (destructive) interference of the wave functions of opposite sign (maroon and green) results in polar HOMO and HOMO-2 at $\boldsymbol{E}$=0.08 V/Å, of opposite electrical polarization. We find a similar effect between the spin-down LUMO and LUMO+2, shown in Fig. 4(c). For $\boldsymbol{E}$>0.08 V/Å, each spin-polarized polar HOMO and LUMO energy evolves according to the Stark effect, crossing the Fermi level at a different field, loosing (gaining) a majority- (minority-) spin electron and giving rise to a discontinuous change of the MO energies. Thus, the net magnetization decreases until it eventually vanishes when the system undergoes a transition to the NM state. For example, the n=8(5)-DGN having an excess of six (two) majority-spin electrons and S_z=3(1) at zero field, undergoes three (one) Fermi-level crossings before entering the NM state.

The current success of silicon electronics is based on having a robust building block that allows for large-scale integration. We have demonstrated the possibility of an alternative carbon-based building block, analog to the transistor, which opens interesting prospects for developing distinct allcarbon spin electronics. DGNs are intriguing systems that harness the magnetism and magnetoelectro behavior known to arise in finite graphene nanostructures, which can be controlled selectively by an electric field. By design, a DGN exhibits well defined magnetic states and allows the modulation of its electrical conductance by electrically varying its local magnetism.

Acknowledgments

The work at CSUN was supported by NSF-PREM Grants No. DMR-00116566 and No. DMR-0958596, and by NIH Grants No. 3SC3GM084838-02S1 and No. 1SC3GM084838-02.

References

1. Castro Neto AH, Guinea F, Peres NMR, Novoselov KS, Geim AK. Rev. Mod. Phys. 2009; 81:109.
2. Du X, Skachko I, Barker A, Andrei EY. Nat. Nanotechnol. 2008; 3:491. [PubMed: 18685637]
3. Bolotin KI, Sikes KJ, Jiang Z, Klima M, Fudenberg G, Hone J, Kim P, Stormer HL. Solid State Commun. 2008; 146:351.
4. Katsnelson MI, Novoselov KS, Geim AK. Nat. Phys. 2006; 2:620.
5. Son YW, Cohen ML, Louie SG. Nature (London). 2006; 444:347. [PubMed: 17108960]
6. Rudberg E, Salek P, Luo Y. Nano Lett. 2007; 7:2211. [PubMed: 17602536]
7. Hod O, Peralta JE, Scuseria GE. Phys. Rev. B. 2007; 76:233401.
8. Ezawa M. Phys. Rev. B. 2007; 76:245415.
9. Hod O, Barone V, Scuseria GE. Phys. Rev. B. 2008; 77:035411.
10. Hod O, Barone V, Peralta JE, Scuseria GE. Nano Lett. 2007; 7:2295. [PubMed: 17628112]
11. Kan E-J, Li Z, Yang J, Hou JG. Appl. Phys. Lett. 2007; 91:243116.
12. Fernández-Rossier J, Palacios JJ. Phys. Rev. Lett. 2007; 99:177204. [PubMed: 17995364]
13. Wang WL, Meng S, Kaxiras E. Nano Lett. 2008; 8:241. [PubMed: 18052302]

14. Wang WL, Yazyev OV, Meng S, Kaxiras E. Phys. Rev. Lett. 2009; 102:157201. [PubMed: 19518670]
15. Trauzettel B, Bulaev DV, Loss D, Burkard G. Nat. Phys. 2007; 3:192.
16. Westervelt RM. Science. 2008; 320:324. [PubMed: 18420920]
17. Ponomarenko LA, Schedin F, Katsnelson MI, Yang R, Hill EW, Novoselov KS, Geim AK. Science. 2008; 320:356. [PubMed: 18420930]
18. Koskinen P, Malola S, Häkkinen H. Phys. Rev. Lett. 2008; 101:115502. [PubMed: 18851294]
19. Jia X, Hofmann M, Meunier V, Sumpter BG, Campos-Delgado J, Romo-Herrera JM, Son H, Hsieh Y-P, Reina A, Kong J, Terrones M, Dresselhaus MS. Science. 2009; 323:1701. [PubMed: 19325109]
20. Girit CÖ, Meyer JC, Erni R, Rossell MD, Kisielowski C, Yang Li, Park C, Crommie MF, Cohen ML, Louie SG, Zettl A. Science. 2009; 323:1705. [PubMed: 19325110]
21. Soler JM, et al. J. Phys.: Condens. Matter. 2002; 14:2745.
22. Perdew JP, Burke K, Ernzerhof M. Phys. Rev. Lett. 1996; 77:3865. [PubMed: 10062328]
23. For high field, higher order effects may be predominant in the shift of the nonfrontier levels, though the screening of the frontier ones. For instance, the HOMO↓ shifts opposite to what is expected from the Stark effect due to the screening by the HOMO↑, which creates an effective field opposite to the applied field.

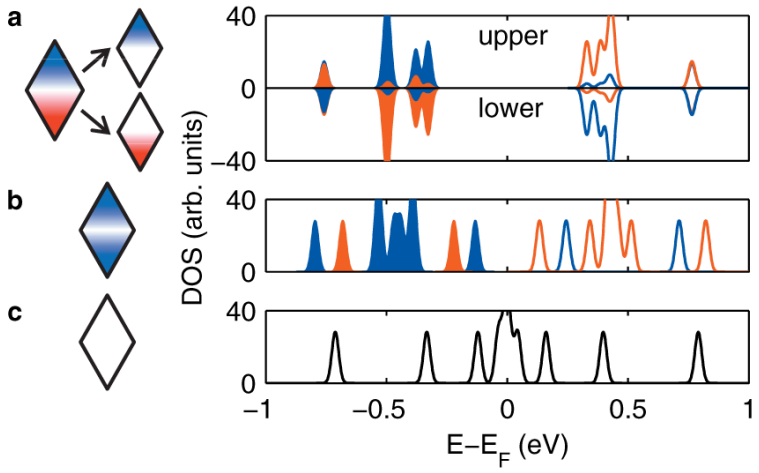

FIG. 1.

(Color) (a) DOS for the AF state, projected on the upper and lower triangular subunits of the *n*=8-DGN; the blue (red) curves denote the spin-up (spin-down) states. [(b) and (c)] DOS for the FM and NM (black curves) states, respectively. The left panels denote schematically the up (blue) and down (red) spin densities of the DGN, where white indicates the absence of magnetization. A broadening of 20 meV was applied to the eigenenergies to produce a smooth DOS.

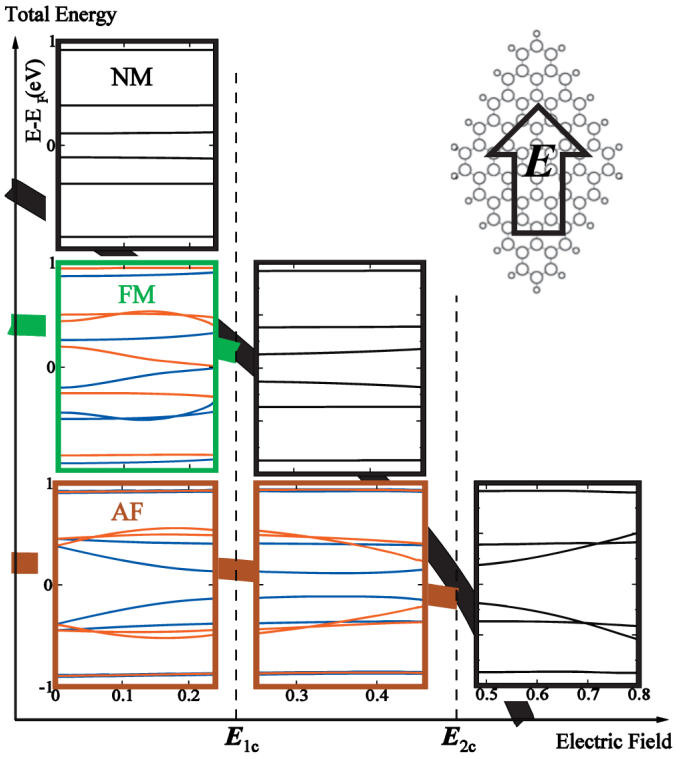

FIG. 2.

(Color) Field variation in frontier MO energies for the AF (brown panels), FM (green panels), and NM (black panels) states of the *n*=5-DGN, in the low- ($\boldsymbol{E}<\boldsymbol{E}_{1c}$), intermediate- ($\boldsymbol{E}_{1c}<\boldsymbol{E}<\boldsymbol{E}_{2c}$), and high-field ($\boldsymbol{E}>\boldsymbol{E}_{2c}$) regimes, where the DGN exhibits three, two, and one states, respectively. The thick brown, green, and black curves denote schematically the field variation in the corresponding total energy for the AF, FM, and NM states, respectively. The vertical dashed lines denote the critical fields $\boldsymbol{E}_{1c}\approx 0.25$ V/Å and $\boldsymbol{E}_{1c}\approx 0.47$ V/Å, where the DGN undergoes FM→NM and AF→NM transitions. The thin blue, red, and black curves denote spin-up, spin-down, and nonpolarized MO energies. The inset shows the hydrogen-terminated (small circles) edges with the field applied along the main diagonal.

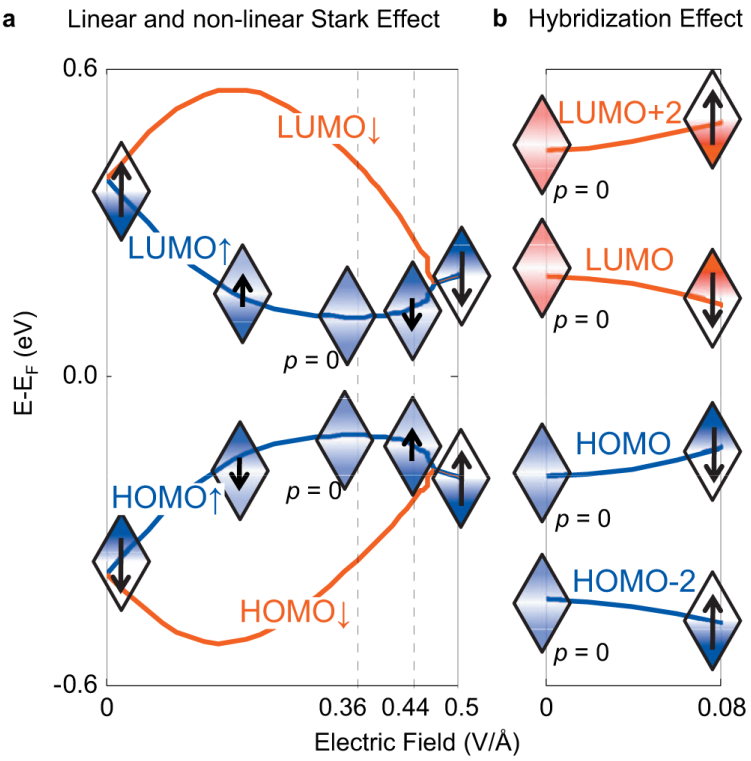

FIG. 3.

(Color) (a) Field variation in spin-up frontier MO energies (blue curves) for the AF state of the *n*=5-DGN. Schematic field evolution of the corresponding frontier MO spin-up density (blue), where white denotes the absence of magnetization. The linear (nonlinear) Stark effect occurs for $\boldsymbol{E}$<0.10 V/Å ($\boldsymbol{E}$>0.10 V/Å), where the MOs polarization, $\vec{p}$, denoted by black arrows, is independent of (dependent on) field. The low-field polarization of the spin-up polar frontier MO, localized on opposite triangles, decreases with increasing field until it vanishes at 0.36 V/Å, where the field slope of the energies also vanishes and the MO become symmetric in both triangles. At ≈0.44 V/Å, the MO polarization and the field slope of the energies reverses. (b) Low-field (<0.08 eV/Å) *hybridization*-induced variation in spin-up (blue) and spin-down (red) frontier MO energies in the FM state. The field evolution of the corresponding spin-up and spindown densities is shown also schematically. Hybridization of non-polar MO of opposite parity (not visible) leads to repulsion of the spin-down LUMO and LUMO+2 energies and the spin-up HOMO and HOMO-2 energies, and the formation of polar bonding and antibonding MO of opposite polarization.

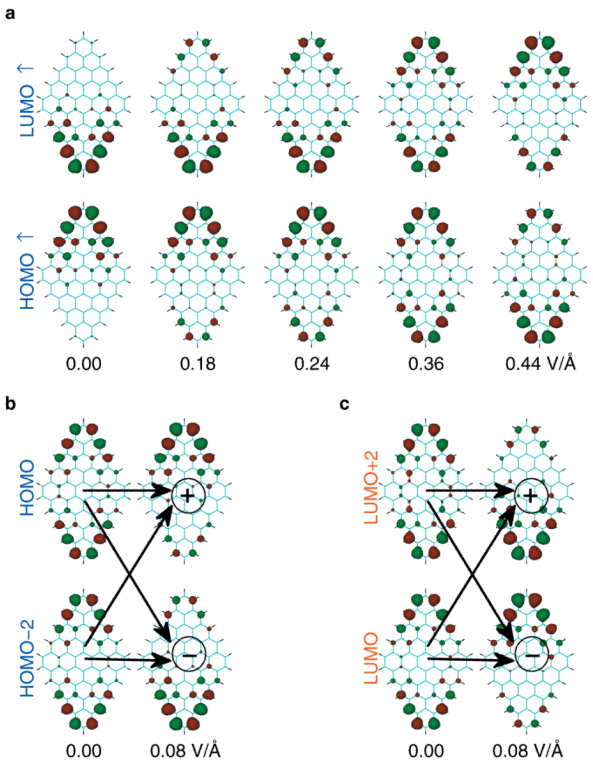

FIG. 4.

(Color) (a) Field variation in the HOMO↑ and LUMO↑ for the AF configuration of the *n*=5 DGN, localized on the upper and lower triangles, respectively. The zero-field MO are polar with the HOMO↑ (LUMO↑) having a dipole moment antiparallel (parallel) to the electric field applied along the larger diagonal of the diamond. [(b) and (c)] Low-field (≤0.08 V/Å) variation in the spin-up HOMO and HOMO-2, and of the spin-down LUMO and LUMO+2, respectively, for the FM state. The arrows indicate the bonding (+) and antibonding (−) hybridization of nonpolar MO of *opposite* parity. The maroon and green isosurfaces (0.025 a.u.) denote opposite sign of the wave functions.